CHAPTER VI
RESULT AND DISCUSSION

4.1 Characterization of Cellulose Fibers derived From Banana Trunks

4.1.1 Morphological Analysis

The SEM image of cellulose fiber, which was prepared from inner core of banana trunk, illustrates that the cellulose fiber exhibited long and slender microfibril structure, and the individual or aggregated fragments can be seen as shown in Figure 4.1. The width and length were estimated from the selected SEM images. The average length and diameter of the cellulose fibers were found to be 0.49 mm and 3.16 μm, respectively, corresponding to the aspect ratio (L/D) of about 155.

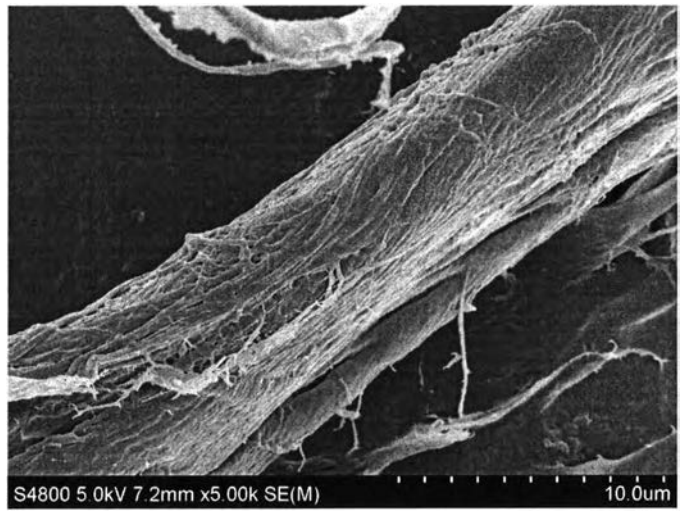

Figure 4.1 SEM image of cellulose fibers obtained from acid hydrolysis of banana trunks.

4.1.2 Chemical Analysis

The chemical structures of the original banana trunks and the resulting cellulose fibers were investigated with the use of the FTIR spectroscopy. As shown in Figure 4.2, the FTIR spectra of both original banana trunks and prepared cellulose fibers show a broad band of the OH-stretching in a wavenumber range of 3650 cm^{-1} to 3000 cm^{-1}. A removal of lignin after chemical treatment is confirmed by a loss of characteristic peak at 1595 cm^{-1} which can be assigned to the C=C bonds in benzene ring of lignin, as shown in the FTIR spectrum of prepared cellulose fibers. However, the as-prepared cellulose fiber also still contains some lignin, as indicated by the existence of the FTIR peaks at 1675 cm^{-1} which correspond to the acetyl and uronic ester groups of hemicellulose or the ester linkage of carboxylic group of ferulic and p-coumaric acids of lignin and/or hemicellulose (Sain and Panthapulakkal, 2006; Sun, Xu, Sun, Fowler and Baird, 2005). Other two peaks at 1061 and 897 cm^{-1} are associated with the C–O stretching and C–H rock vibrations of cellulose (Alemdar and Sain, 2008), which appeared in both of the spectra.

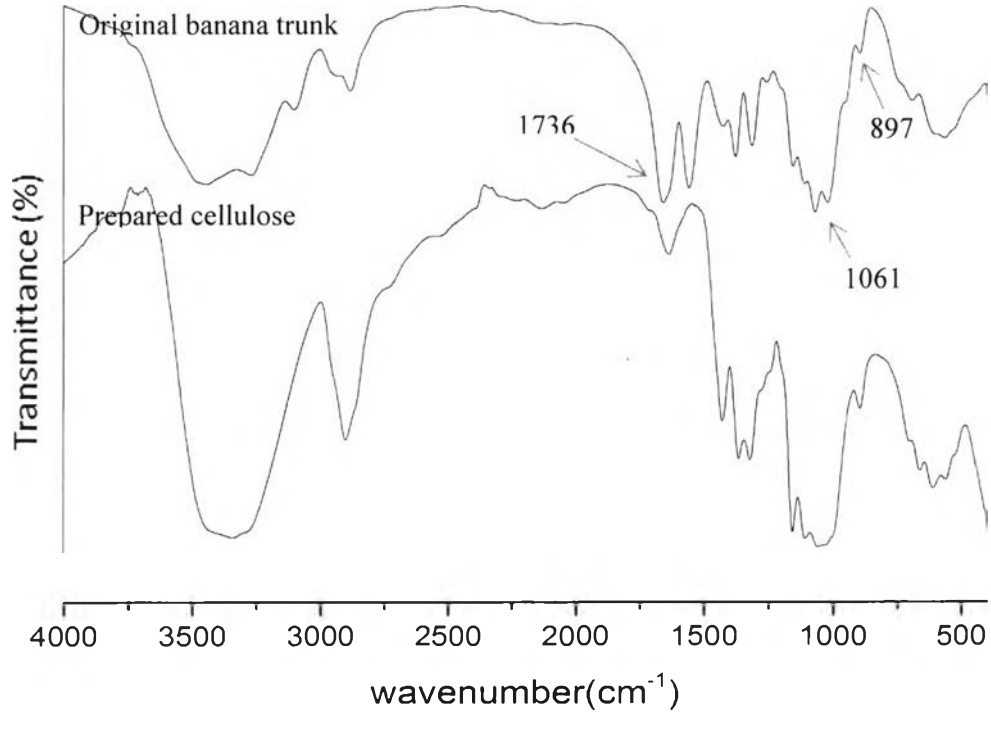

Figure 4.2 FTIR spectra of original banana trunks and prepared cellulose fibers.

4.1.3 Thermogravimetric Analysis

The thermal degradation behavior of the native banana trunks, and the resulting cellulose fibers were determined. As shown in Figure 4.3, the TGA of native banana trunks showed the weight loss in five stages. The initial stage ranged between 74°C and 228°C that might correspond to the loss of the adsorbed water. The second stage of the weight loss started at 228°C to 308°C is due to the degradation of hemicellulose. Thermal decomposition of cellulose started at about 308◦C, followed by two major weight losses during the decomposition of lignin, which are essentially completed at about 855◦C. In comparison with native cellulose, the TGA of cellulose fibers derived from banana trunks showed the weight loss only in three stages. The first region in the temperature regime of 41°C to 202°C is due to the evaporation of weakly bound water. The second transition region at around 202°C to 322°C is due to degradation of residual hemicellulos. The third stage of weight loss occurred at about 322°C, perhaps due to the decomposition of cellulose, with a weight loss of around 84% (Yang *et al.*, 2007). The results indicated that hemicellulose and lignin were removed from native banana trunks after alkali and acid treatment.

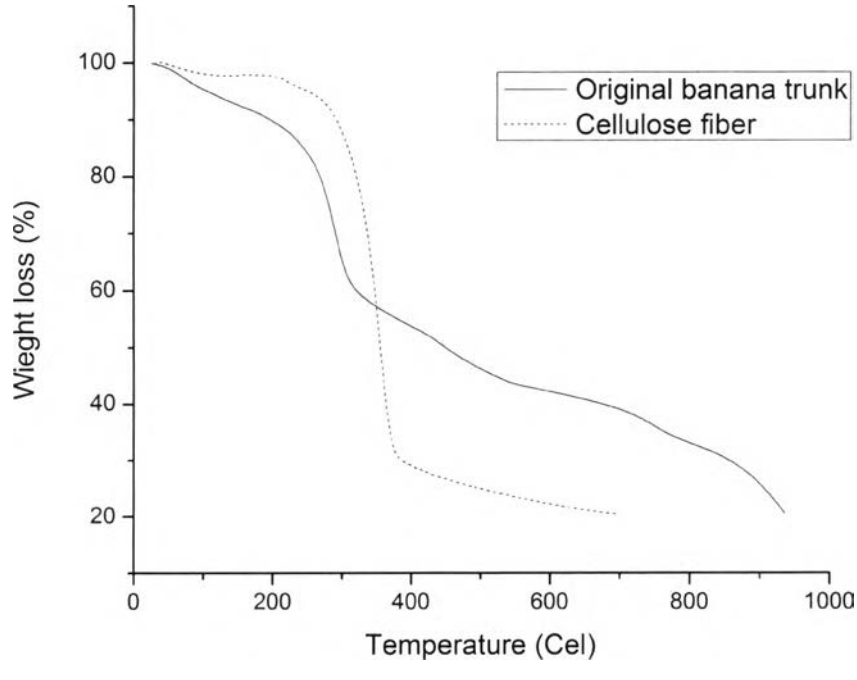

Figure 4.3 The thermogravimetric analysis of original banana trunk and cellulose fibers.

4.2 Characterization of DBD Plasma-treated Cellulose Sheets

4.2.1 Effect of DBD Plasma Treatment Time on Water Contact Angle on Cellulose sheets

The hydrophilicity of DBD plasma-treated banana cellulose-based sheet was characterized by water contact angle measurement. The effect of DBD plasma treatment time on the water contact angle of the plasma-treated banana cellulose sheets was determined. Obviously, Figure 4.4 shows that the water contact angle drastically decreased from 55.7° to 11.3° as the DBD plasma treatment time increased from 0 s to 5 s. A constant water contact angle of around 10° at the treatment time longer than 5 s implied a saturation state of surface hydrophilicity. The result indicated that the DBD plasma treatment led to an increase in the surface hydrophilicity of the plasma-treated cellulose sheets. This should be mostly likely due to the presence of new polar functional groups on the plasma-treated surface induced by the active species generated by the air plasma, especially oxygen-based species and charged species, which are very reactive (Esena *et al.* 2008).

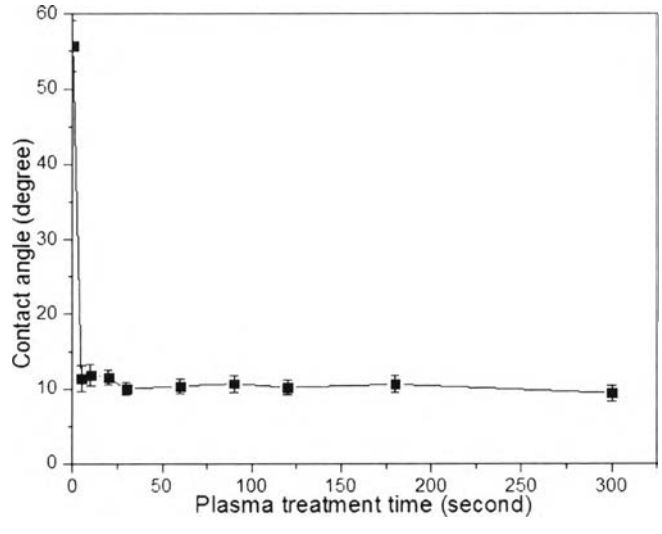

Figure 4.4 Effect of plasma treatment time on water contact angle on cellulose sheets.

4.2.2 Effect of DBD Plasma Treatment Time on Surface Chemical Composition of Cellulose Sheets

The surface chemical composition of DBD plasma-treated cellulose sheet was investigated by using the ATR-FTIR technique. The ATR-FTIR spectra of the cellulose sheets before and after the DBD plasma treatment was determined as shown in Figure 4.5. After the DBD plasma treatment, the new characteristic peaks appearing at the wavenumbers of 1633 cm^{-1} and 1718 cm^{-1} corresponding to COO– asymmetrical stretching vibration and C=O stretching vibration, respectively (Ragojanu *et al.*, 2010). The intensity of the new peaks was also found to increase with increasing the DBD plasma treatment time, implying a higher amount of the new oxygen-containing functional groups at a longer plasma treatment time.

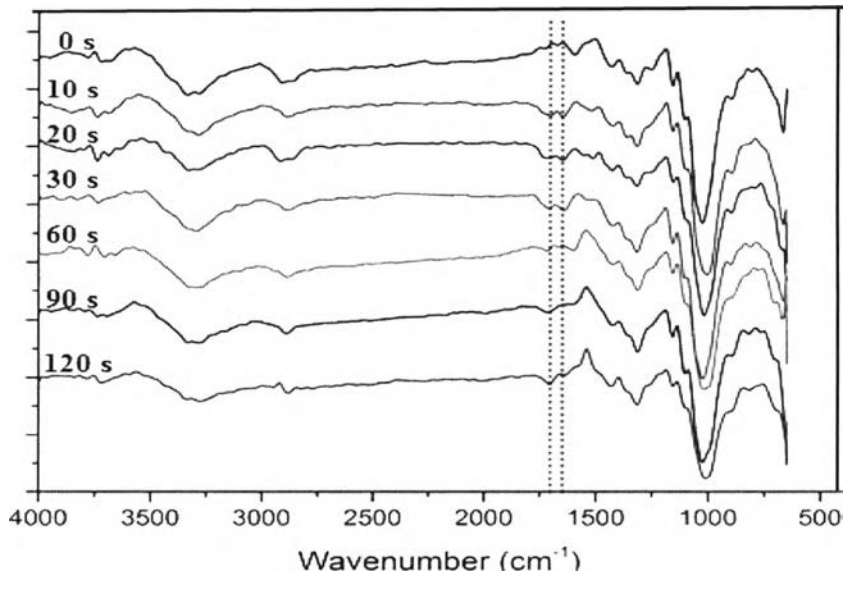

Figure 4.5 ATR-FTIR spectra of cellulose sheets at different DBD plasma treatment time.

Moreover, the chemical composition of treated-cellulose sheets was further examined using the XPS technique. Figures 4.6 (a) and (b) show the C(1s) spectra of untreated cellulose sheets and plasma-treated cellulose sheets at 30 s. The result shows that the chemical composition of untreated cellulose sheets is altered after the plasma treatment which can be observed from three main peaks. The peak at

283.3, 285.0 and 286.4 eV was attributed to C-C/C-H, C-O and C-O-C/C=O bond (Rjeb *et al.,* 2004). The last peak at 287.7 eV was attributed to O-C=O bond (Morent *et al.*, 20107). As shown in table 4.1, the percentage of oxygen- containing polar group which are C-O, C-O-C/C=O and O-C=O are increased as increasing the plasma treatment time whereas the percentage of C-C/C-H was decreased. It might be implied that the DBD plasma changed the surface chemistry of cellulose sheets by decomposition of polymer chains and oxidation reactions forming aldehyde and carboxylic acid/carboxylate groups lead to the formation of the oxygen-containing polar functional groups, relating to an increase in the C-O-C/C=O and O-C=O bond (Calvimontes *et al.*, 2011). These results were in agreement with the FTIR results.

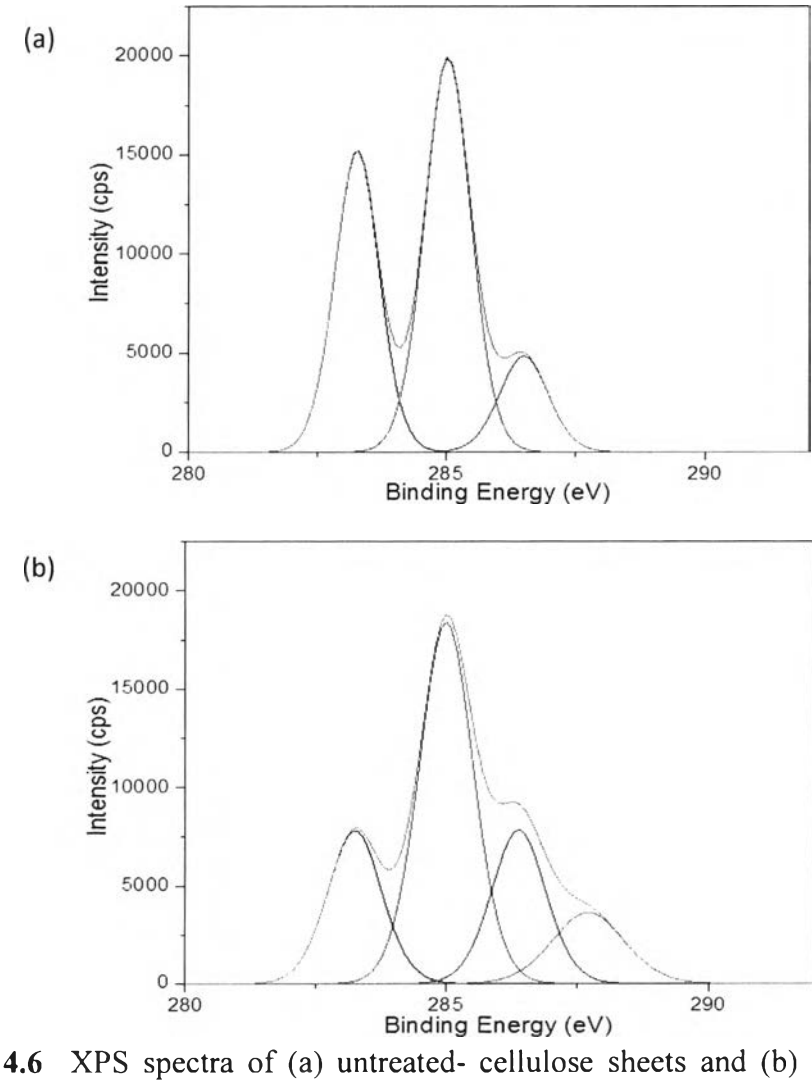

Figure 4.6 XPS spectra of (a) untreated- cellulose sheets and (b) plasma-treated cellulose sheets at 30 s.

Table 4.1 Effect of plasma treatment time on the percentage of chemical composition

Treatment time (s)	Percentage of chemical composition			
	283.3 eV C-C/C-H	**285.0 eV C-O**	**286.4 eV C-O-C/C=O**	**287.7 eV O-C=O**
0	37	50.2	12.9	-
10	21.8	56.1	18.1	4.1
30	20.2	47.3	20.2	12.3

4.2.3 Effect of DBD Plasma Treatment on Crystallinity of Cellulose Sheets

The characteristic diffractions of untreated and 30 s DBD plasma-treated cellulose sheets are shown in Figure 4.7. Clearly, it can be seen that both samples showed the diffraction peak 2θ at 14.7, 16.4, 22.7, characteristic of cellulose crystal assignments of the 1 $\bar{1}$ 0, 1 1 0, and 2 0 0 planes, respectively (Lu *et al.*, 2012). It may be implied that the DBD plasma modification does not change the degree of crystallinity, does not eliminate crystalline domains or form new crystalline species (Calvimontes *et al.*, 2011).

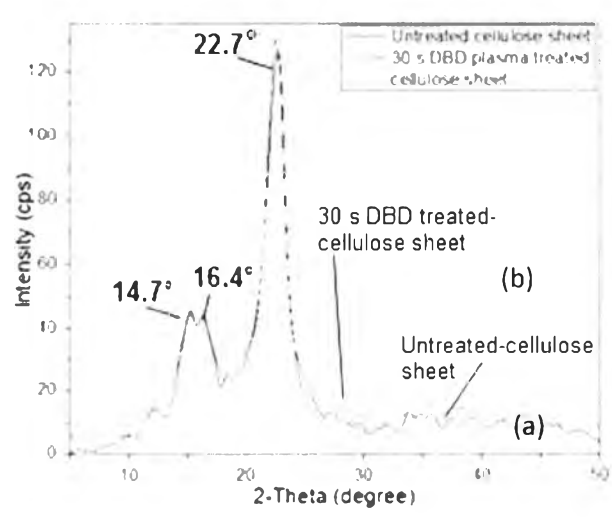

Figure 4.7 XRD pattern of (a) untreated and (b) 30 s DBD plasma treated cellulose sheets.

4.3 Characterization of Natural Rubber-coated Cellulose Sheets

4.3.1 Effect of NR Coating on Surface Morphology of Cellulose Sheets

Figure 4.8 (a) and (b) shows the surface morphology of untreated cellulose sheets and NR-coated cellulose sheets, respectively. After NR coating, it can be seen that the surface of cellulose was smoother due to that surface was covered with a thin NR layer (Samanta *et al.*, 2012).

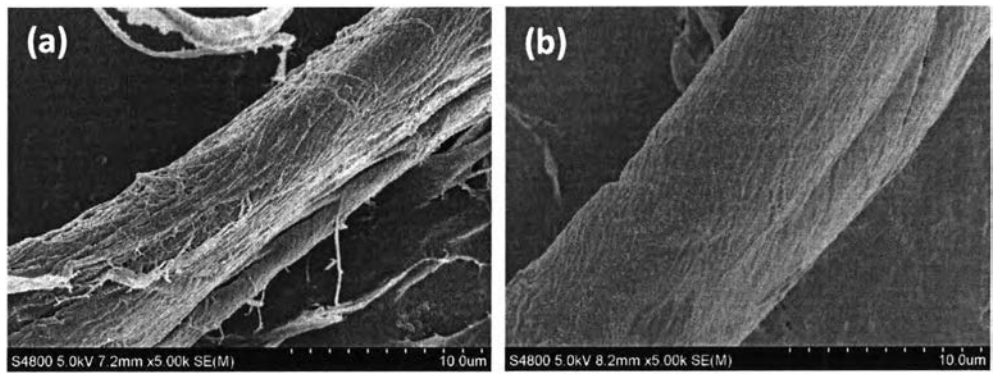

Figure 4.8 SEM images of (a) untreated cellulose fiber and (b) NR-coated cellulose fibers.

4.3.2 Effect of NR Coating on Thickness of Cellulose Sheets

The thickness of the cellulose sheets was also determined after the NR coating. As shown in table 4.2, the coated NR on plasma-treated cellulose sheets did not affect the thickness of cellulose sheets. This is possibly because the coated NR on cellulose surface was very thin layer.

Table 4.2 Thickness of untreated and NR-coated cellulose sheets

Samples	Thickness (μm)
Untreated cellulose sheet	102.5±17.64
A	103.1±13.39
B	102.2±11.52
C	105.3±16.67

4.3.3 Effect of DBD Plasma Treatment Time on The Amount of coated NR

The amount of NR coated on cellulose sheet was quantitatively determined by using alkene bromination. The color changing of Br_2 after it reacted with double bond of natural rubber-coated on cellulose sheet surface was determined by UV-Visible Spectroscopy. Figure 4.9 shows the effect of DBD plasma treatment time on the amount of NR coated on cellulose sheet. The concentration of Br_2 reacted with coated NR increased with increasing the plasma treatment time from 0 s to 30 s and then decreased at a plasma treatment time greater than 30 s. Since active species can be increased with increasing plasma treatment time, these species more reacted with double bond of NR resulting in increasing amount of NR-coated on cellulose surface. However, rubber is a very long chain polymer that can obstruct reaction of other chain. When free radicals on cellulose surface are too much, a rubber chain might react with several free radicals on cellulose surface resulting in decreasing amount of double bond on NR-coated on cellulose surface and water contact angle. Therefore, the optimum time for the DBD plasma treatment of cellulose sheet was selected at 30 s.

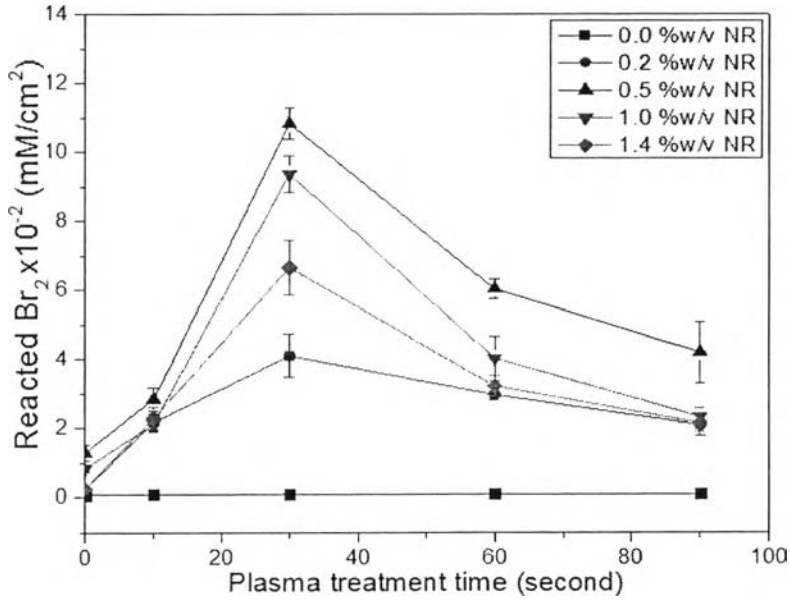

Figure 4.9 Effect of DBD plasma treatment time on amount of coated NR.

4.3.4 Effect of NR Concentration on The Amount of NR-coated on Cellulose Sheets

The effect of NR Concentration on amount of NR coated on cellulose sheets was studied. As shown in Figure 4.10, the amount of coated NR increased with increasing the NR concentration from 0.2 %w/v to 0.5 %w/v and then decreased at a NR concentrations greater than 0.5 %w/v. Since viscosity of NR solution increased with increasing the NR concentration, as shown in Figure 4.11, the reaction between NR and cellulose surface was difficult to occur. The result revealed that the optimum NR concentration for coating on cellulose sheets was 0.5 %w/v.

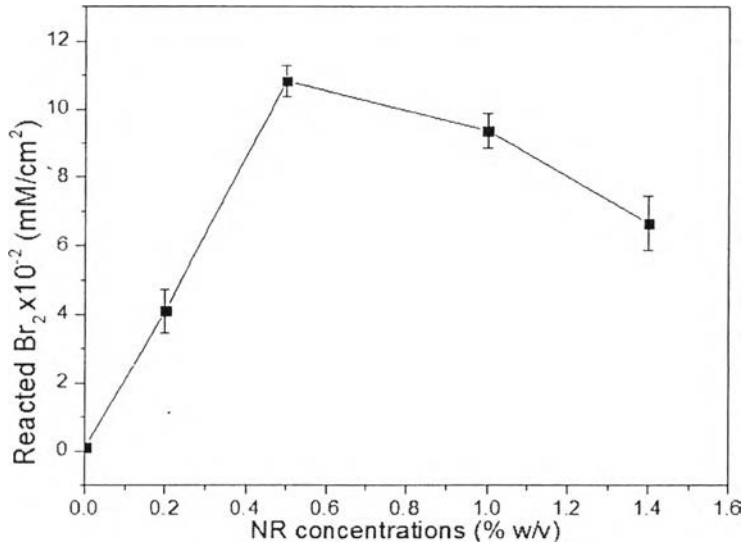

Figure 4.10 Effect of NR concentration on amount of coated NR on cellulose sheets.

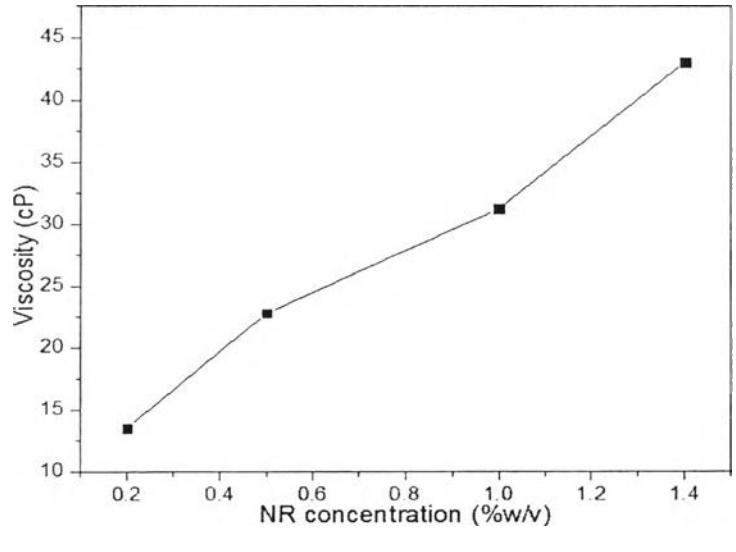

Figure 4.11 Effect of NR concentration on viscosity of NR solution.

4.3.5 Effect of NR Coating on Water Contact Angle on Cellulose Sheets

The water contact angle of the cellulose sheets was determined after the NR coating. As shown in Figures 4.12, the water contact angle of cellulose sheet increased after coated with NR. The result indicated that an increase in the plasma treatment time from 0 s to 30 s and NR concentration from 0.2 %w/v to 0.5 %w/v increased the water contact angle of the NR-coated cellulose sheets. However, at a plasma treatment time greater than 30 s and NR concentration greater than 0.5 %w/v, water contact angle of the NR-coated cellulose sheets started to decrease. This is possibly because hydrophobicity of NR coated on cellulose sheet was decreased when plasma treatment time greater than 30 s. Moreover, NR coating capability on cellulose surface was decreased when NR concentration was higher than 0.5%w/v.

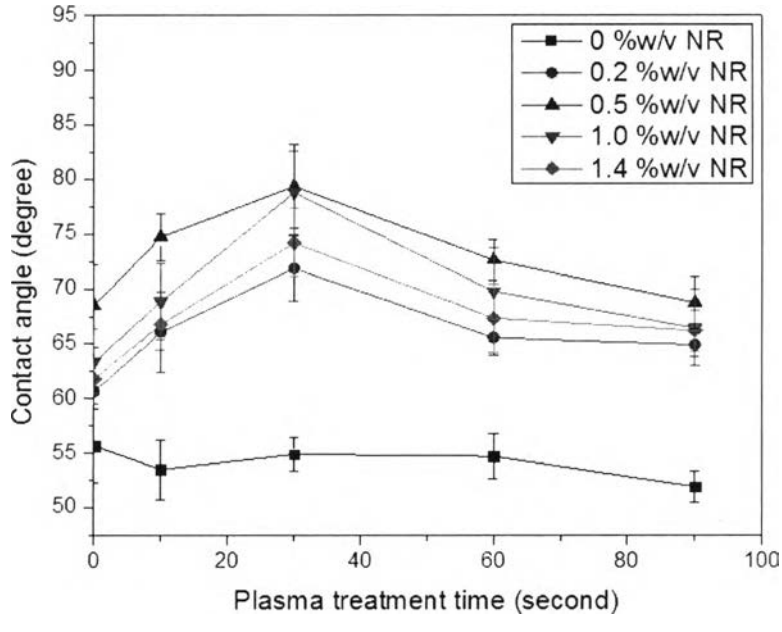

Figure 4.12 Effect of NR-coated cellulose sheets on water contact angle.

4.3.6 Effect of NR Coating on Thermal Properties of Cellulose Sheets

Thermal properties of NR-coated cellulose sheets were determined with the use of differential thermal analysis (DTA). Figure 4.13 shows the effect of NR coating on thermal properties of cellulose sheets. From thermal analysis of untreated cellulose-based sheets and NR-coated treated-cellulose-based at the heating rate of 10°C/min, it indicated that the thermal stability of cellulose sheets slightly increased

after NR coating, and NR-coated DBD treated cellulose sheet at 30 s has the highest thermal stability. It might be implied that coating ability of NR on cellulose sheet is highest when plasma treatment time is 30s.

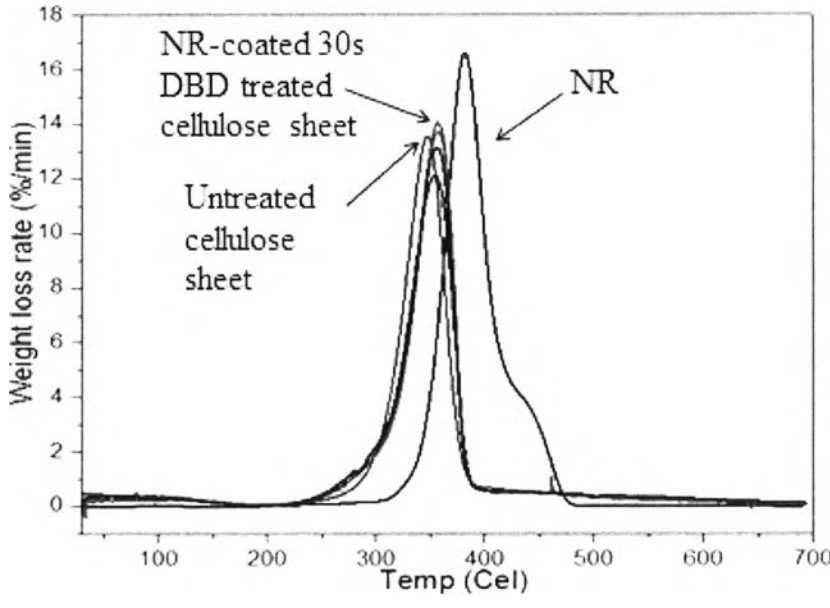

Figure 4.13 Effect of NR-coated cellulose sheets on thermal stability.

4.3.7 Effect of NR Coating on Crystallinity of Cellulose Sheets

Crystallinity of NR-coated cellulose sheets was determined with the use of wide angle x-ray diffraction (WAXD) analysis. Figure 4.14 shows the characteristic diffractions of 30 s DBD plasma treated and NR-coated cellulose sheets. From the result, it indicated that the crystallinity of cellulose sheets did not change after NR coating, but the intensity of the diffraction signal decreased. It might be implied that NR that is amorphous was coated on cellulose surface.

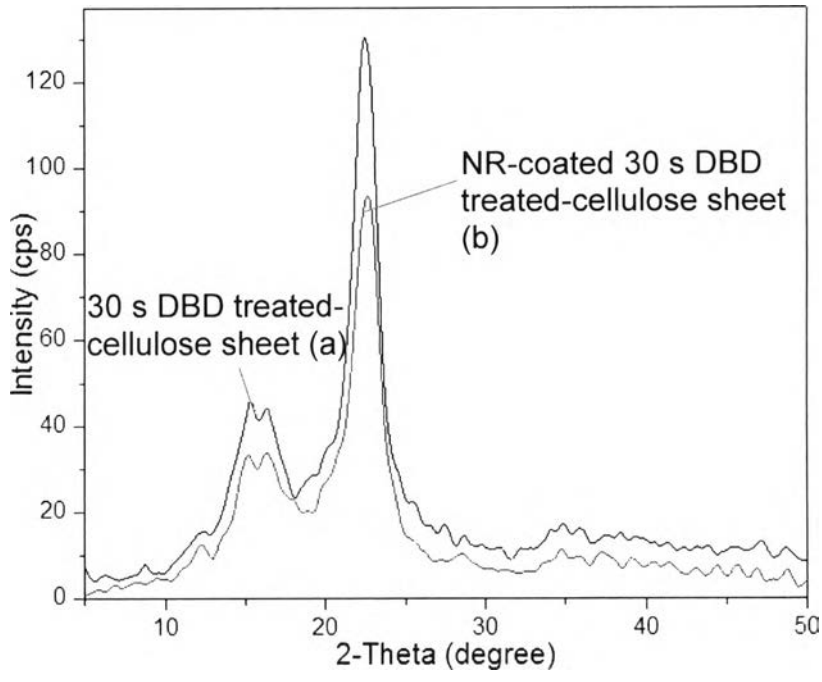

Figure 4.14 XRD pattern of (a) 30 s DBD plasma treated and (b) NR-coated cellulose sheets.

4.3.8 Effect of Number of NR coating Cycles on The Amount of NR-coated on Cellulose Sheets and Water Contact Angle

The effect of number of NR coating cycles on amount of NR coated on cellulose sheet and water contact angle was studied at the optimum time for the DBD plasma treatment and NR concentrations. As shown in Figure 4.15, the amount of coated NR and water contact angle increased with increasing the NR coating cycle before remaining constant at a NR coating cycle greater than 2 times. The result revealed that the saturated amount of NR coated on plasma-treated cellulose sheets was obtained after the samples were coated for two times.

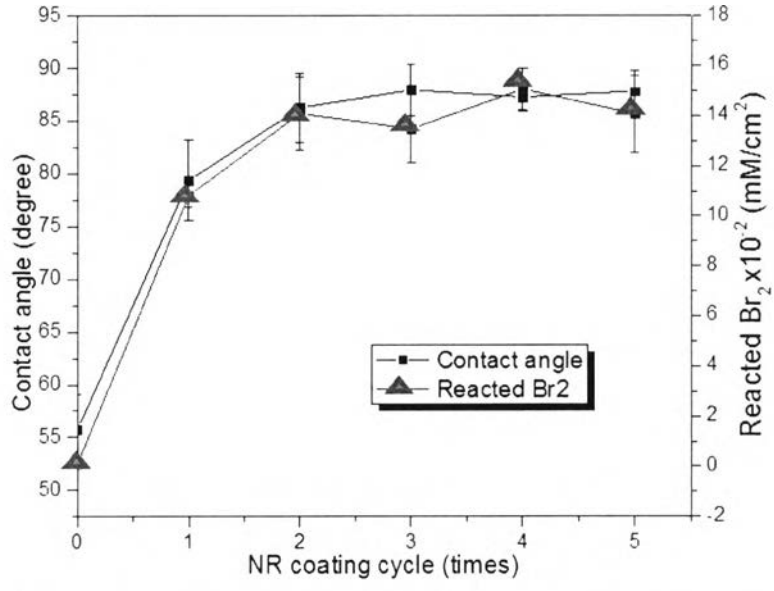

Figure 4.15 Effect of number of coating cycles on amount of NR coated and water contact angle on cellulose sheets.

4.3.9 Effect of ZnO on The Amount of NR coated on Cellulose Sheets

The effect of ZnO on amount of NR coated on cellulose sheet was studied at the optimum NR concentrations as shown in Figure 4.16. When ZnO was used, the amount of coated NR increased with increasing the plasma treatment time from 0 s to 60 s before decreasing at a plasma treatment time greater than 60 s. The result indicated that NR coating ability on cellulose sheets was improved with the aid of ZnO. Moreover, when cellulose sheet and NR were treated with DBD plasma at the same time (B), it found that NR coating ability was better than treated cellulose sheet before dipping in NR solution (A). It may be implied that cellulose can react with NR better in DBD plasma.

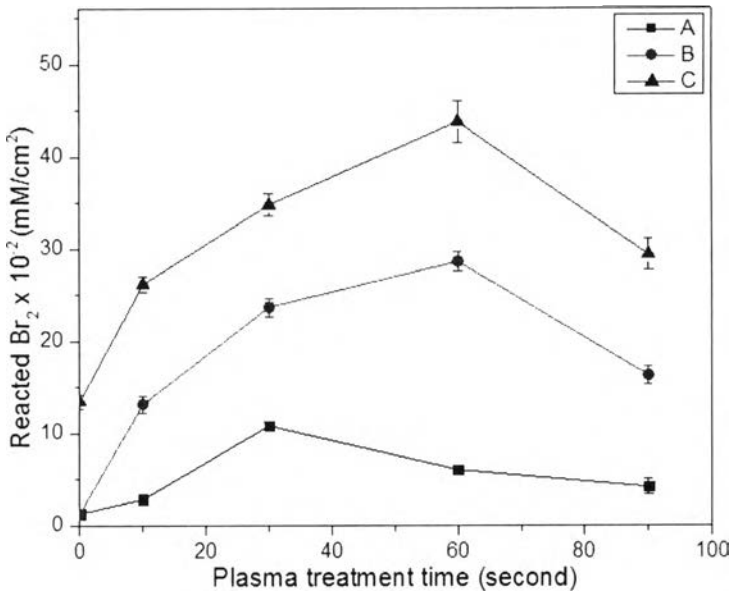

Figure 4.16 Effect of ZnO on amount of NR coated on cellulose sheets.

4.3.10 Effect of ZnO on Water Contact Angle on Cellulose Sheets

The effect of ZnO on water contact angle on cellulose sheets was also studied at the optimum NR concentrations. As shown in Figure 4.17, the water contact angle on cellulose sheets increased with using ZnO. The result revealed that the highest water contact angle on cellulose sheet was about 124.43°

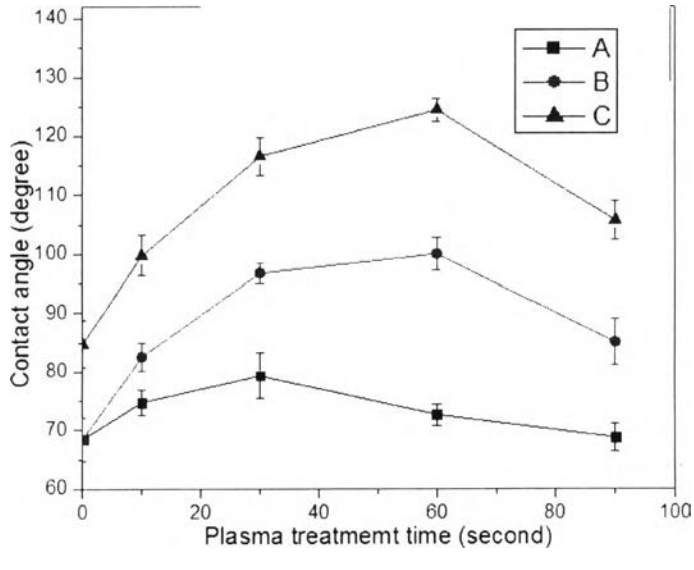

Figure 4.17 Effect of ZnO on water contact angle on cellulose sheets.

4.3.11 Effect of $Zn(NO_3)_2$ Concentration on The Amount of NR-coated on Cellulose Sheets and Water Contact Angle

The effect of $Zn(NO_3)_2$ concentration on the amount of NR-coated on cellulose sheets and water contact angle was studied at the optimum plasma treatment time. As shown in Figure 4.18, the amount of NR-coated on cellulose sheets and water contact angle increased with increasing the $Zn(NO_3)_2$ concentration from 0.05 M to 0.5 M before remaining constant at a $Zn(NO_3)_2$ concentration greater than 0.5 M. The result revealed that the optimum $Zn(NO_3)_2$ concentration for ZnO coating on cellulose sheets was 0.5 M.

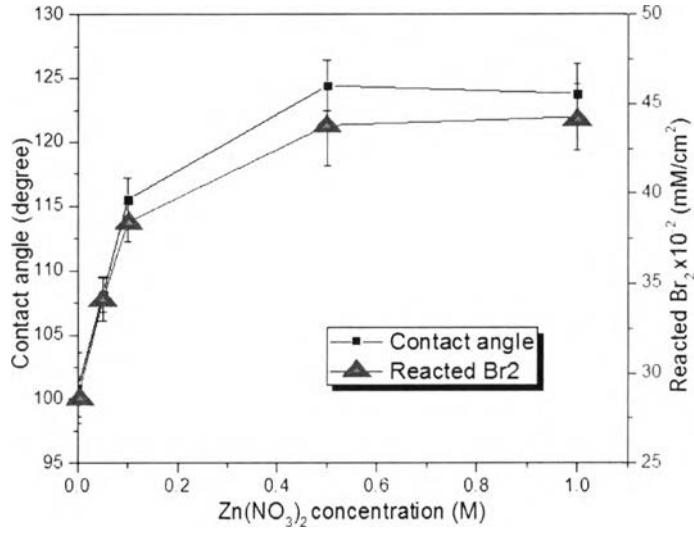

Figure 4.18 Effect of $Zn(NO_3)$ concentration on amount of coated NR and water contact angle on cellulose sheets.

4.4.12 The Distribution of ZnO Deposition on cellulose sheets

The distribution of ZnO deposition on cellulose sheet was also observed with the use of the SEM-EDX technique. From Figures 4.19, the SEM micrographs clearly show a homogeneous distribution of ZnO particles on the cellulose surface.

Figure 4.19 SEM-EDX images of Zn atom distributed on NR/ZnO-coated DBD plasma-treated cellulose surface.

4.3.13 Effect of NR Coating on Chemical Composition of Cellulose Sheets

The chemical bonding between the plasma treated-cellulose sheets and the coated NR was verified by the XPS technique. Figure 4.20 (a) and (b) shows C 1s XPS spectra of NR-coated and NR/ZnO-coated DBD plasma-treated cellulose sheets, respectively. The result indicated that the chemical composition of NR-coated DBD plasma-treated cellulose sheets showed four main peaks. The peak at 283.3, 285.0 and 286.4 eV was attributed to C-C/C-H, C-O and C-O-C/C=O bond. The last peak at 287.7 eV was attributed to O-C=O bond (Rjeb *et al.*, 2004). The result shows that the chemical composition of untreated cellulose sheets is altered after coating with NR. From table 4.3, it can be seen that the NR-coated cellulose sheet resulted in an increase of the C-C/C-H groups and a corresponding decrease of oxygen containing species.

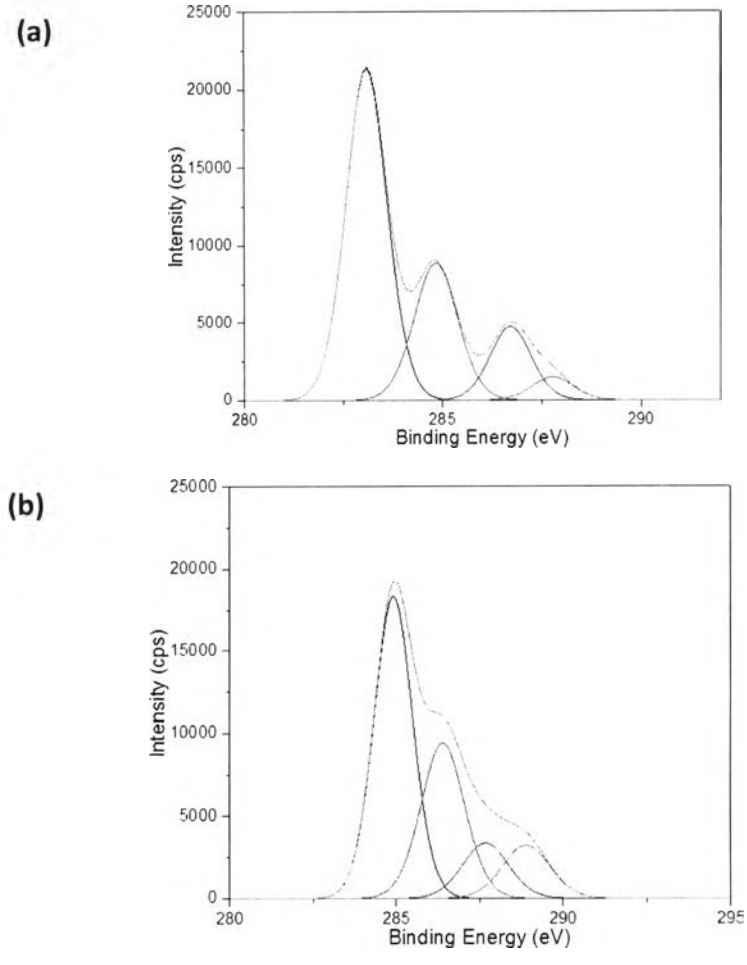

Figure 4.20 XPS spectra of (a) NR-coated (A) and (b) NR/ZnO-coated cellulose sheets (C).

Table 4.3 Effect of NR and ZnO coating on the percentage of chemical composition

Samples	**Atomic concentrations (%)**		
	C 1s	**O 1s**	**Zn 2p**
Cellulose sheet	60.29	39.71	-
NR-coated cellulose sheet (A)	63.61	36.39	-
NR/ ZnO coated cellulose sheet (C)	71.71	24.56	3.73

4.3.14 Water Absorbency Time of NR-Coated DBD Plasma-Treated Cellulose Sheets and Water Contact Angle

To achieve the aim of this study, the water absorbency time of untreated and NR-coated cellulose sheets were determined. Table 4.4 shows the water absorbency time of cellulose sheets at different preparation conditions. The result indicated that the water absorbency time of cellulose sheets increased after NR coating. Moreover, the water absorbency time of cellulose sheets was longer when using ZnO as a crosslinking agent. It may be implied that ZnO improved NR coating ability on cellulose sheets.

Table 4.4 Water droplet absorbency time of the untreated and NR-coated cellulose sheets

Samples	**Water absorbency time (min)**
Untreated cellulose sheet	48±3.00
A	159±4.00
B	185±6.24
C	207±7.94